threshold maintained for dynamically updating population size, crossover and mutation probabilities restricts the unwanted attributes and retains only optimal features in the population. BAGEL supports this process by efficient imputation of missing values. The proposed algorithm is implemented on real datasets. The results show that the classification accuracy obtained on the processed datasets is better than other existing algorithms. DGAFS-MI can thus reduce the burden of clinicians and help them in efficient analysis of microarray datasets.

1. Lee, C.-P. and Leu, Y., A novel hybrid feature selection method for microarray data analysis. *Appl. Soft Comput.*, 2011, **11**, 208–213.
2. Devi Priya, R. and Kuppuswami, S., A genetic algorithm-based approach for imputing missing discrete values in databases. *WSEAS Trans. Inf. Sci. Appl.*, 2012, **9**, 169–178.
3. Pramod Kumar, P., Prahlad, V. and Poh, A. L., Fuzzy-rough discriminative feature selection and classification algorithm with application to microarray and image datasets. *Appl. Soft Comput.*, 2011, **11**, 3429–3440.
4. Fernandez-Navarro, F., Hervás-Martínez, C., Ruiz, R. and Riquelme, J. C., Evolutionary generalized radial basis function neural networks for improving prediction accuracy in gene classification using feature selection. *Appl. Soft Comput.*, 2012, **12**, 1787–1800.
5. Ganesh Kumar, P., Aruldoss Albert Victoire, T., Renukadevi, P. and Devaraj, D., Design of fuzzy expert system for microarray data classification using a novel genetic swarm algorithm. *Exp. Syst. Appl.*, 2012, **39**, 1811–1821.
6. Reboiro-Jato, M., Díaz, F., Glez-Pena, D. and Fdez-Riverola, F., A novel ensemble of classifiers that use biological relevant gene sets for microarray classification. *Appl. Soft Comput.*, 2014, **17**, 117–126.
7. Chen, K.-H., Wang, K.-J., Wang, K.-M. and Angelia, M.-A., Applying particle swarm optimization-based decision tree classifier for cancer classification on gene expression data. *Appl. Soft Comput.*, 2014, **24**, 773–780.
8. Bolon-Canedo, V., Sánchez-Marono, N. and Alonso-Betanzos, A., Distributed feature selection: an application to microarray data classification. *Appl. Soft Comput.*, 2015, **30**, 136–150.
9. Su, Y., Murali, T. M., Pavlovic, V., Schaffer, M. and Kasif, S., RankGene: identification of diagnostic genes based on expression data. *Bioinformatics*, 2003, **19**, 1578–1579.
10. Li, L. *et al.*, A robust hybrid between genetic algorithm and support vector machine for extracting an optimal feature gene subset. *Genomics*, 2005, **85**, 16–23.
11. Zibakhsh, A. and Abadeh, M. S., Gene selection for cancer tumor detection using a novel memetic algorithm with a multi-view fitness function. *Eng. Appl. Artif. Intell*,. 2013, **26**, 1274–1281.
12. Xie, H., Adjusting for nonignorable missingness when estimating generalized additive models. *Biometrika. J.*, 2010, **52**, 186–200.
13. Muthen, B., Asparouhov, T., Hunter, A. and Leuchter, A., Growth modeling with non-ignorable dropout: alternative analyses of the STAR*D antidepressant trial. *Psychol. Meth.*, 2011, **16**, 16–33.
14. Kim, J. K., Calibration estimation using empirical likelihood in survey sampling. *Stat. Sin.*, 2009, **19**, 145–157.
15. Fang, F., Hong, Q. and Shao, J., Empirical likelihood estimation for samples with non-ignorable nonresponse. *Stat. Sin.*, 2010, **20**, 263–280.
16. Devi Priya, R. and Kuppuswami, S., Drawing inferences from clinical studies with missing values using genetic algorithm. *Int. J. Bioinformat. Res. Appl.*, 2014, **10**, 613–627.
17. Kaciroti, N. and Raghunathan, T. E., Bayesian sensitivity analysis of incomplete data using pattern-mixture and selection models through equivalent parameterization. *Ann. Arbor.*, 2009, **1001**, 48109.
18. Siddique, J. and Belin, T. R., Using an approximate Bayesian bootstrap to multiply impute nonignorable missing data. *Comput. Stat. Data Anal.*, 2008, **53**, 405–415.
19. Si, Y., Non-parametric Bayesian methods for multiple imputation of large scale incomplete categorical data in panel studies. Ph D dissertation, Duke University, USA, 2012.

Exposure to particulate matter in different regions along a road network, Jharia coalfield, Dhanbad, Jharkhand, India

Shiv Kumar Yadav and Manish Kumar Jain*

Department of Environmental Science and Engineering,
Indian School of Mines, Dhanbad 826 004, India

Occupational particulate matter (PM) concentrations were measured during November 2014 along a road network in the mining and non-mining areas at Jharia coalfield, Dhanbad, Jharkhand, India. The monitoring was conducted for a week in the peak time using a portable GRIMM (model 1.109) aerosol spectrometer. Measured PM was designated as inhalable, thoracic and alveolic particles for aerodynamic diameter 10–34, 4–10 and less than 4 μm respectively. The main sources of PM along the roadside in the study area were mining operations as well as heavy traffic and resuspension of road dust. Concentration of inhalable particles was maximum at Bankmore (BMO), whereas concentration of thoracic and alveolic particles was maximum at Katrasmore (KMO) in the mining area. Concentration of all three types of particles was minimum at the Indian School of Mines in the non-mining area. The distribution curves of inhalable particles were positively skewed and platykurtic in nature, whereas for thoracic and alveolic particles these curves were positively skewed at all locations, except BMO and also platykurtic in nature, except Godhar (GDR). Contribution of alveoli particle sizes for 0.375

*For correspondence. (e-mail: manishjkm@gmail.com)

and 2.750 μm was observed to be significant in the mining area, whereas thoracic particle size for 5.750 μm and inhalable particle size for 22.500 μm were also observed to be higher in the mining area, except Matkuria check post and Kustaur. The results reveal that residents and local passengers were exposed to a prodigious amount of inhalable, thoracic and alveolic concentrations in the mining area, mostly at BMO, GDR and KMO.

Keywords: Open cast coal mining, particulate matter, road network, traffic volume count.

PARTICULATE matter (PM) is a leading concern for public working and residing along the roadside with respect to health problems such as acute and chronic respiratory symptoms and cardiopulmonary sickness[1–4]. Health problems are also related to size and composition of traffic-related PM with toxicological evidence[5]. Huge amounts of PM are generated in and around surface mining areas due to operational use of high-capacity machines[6–8]. The increasing use of motor vehicles in urban areas is also a major source of generation of PM emission[9,10]. Finer particles in diameter between 0.1 and 1 μm can stay in the atmosphere for days or weeks, and thus are subject to long-range transboundary transport in the air[11]. Earlier studies also showed the impact of PM generated from coal mining on human health, such as lung and kidney diseases, and asthma due to the presence of high concentration of PM and associated pollutants such as heavy metals[12,13]. Several researchers reported that concentration of PM along the roadside due to various activities (automobiles, industries, mines and domestic fuel combustion) is more than the permissible limit provided by the World Health Organization (WHO) and Indian National Ambient Air Quality Standards (NAAQS), which has affected the environment and human health in India[14–21]. Particle size is a significant feature characterizing the properties and behaviour of aerosols. The majority of aerosols have a broad sizes range and their properties depend on variation in particle size. Particles of size range from 0.001 to 100 μm generally remain suspended in the air. Particles small enough may be inhaled through the nose or mouth or both, under average conditions. Suspended particles are commonly classified as follows: less than 4 μm in diameter (alveolic fraction); between 4 and 10 μm diameter (thoracic fraction); greater than 10 μm diameter (inhalable fraction). The upper limit for inhalable particles is not defined. Sometimes PM_{10} can be considered as thoracic fraction for interpretation of result, however it includes both alveolic and thoracic. The respirable particles can reach the alveolar region of the respiratory system; however, about 50% of the particles (4.0 μm) is transmitted through the alveoli. Studies have shown that PM deposits in the respiratory tract depend on the aerosol particle size (e.g. the aerodynamic diameter size distribution), duration of exposure, effi-ciency of the exposure system delivery, ventilation rate of the subject, the species and strain, and other factors[22].

India is the fastest growing and the second heavily populated country in the world, with an estimated population of 1.2 billion[23]. It is facing severe problem of environmental degradation in terms of air pollution in the cities. Dhanbad is also facing the problem of air pollution due to rapid increase in motor vehicles (Jharkhand Transport Department, India), large population (32,988,134; Census of India, 2011) and major coal mining field. Problems of air pollution and generation of dust are more critical in the cities like Dhanbad due to narrow width and poor surface quality of roads. Jharia coalfield (JCF) in Dhanbad has been classified as a non-attainment area[24], because it exceeds NAAQS and air pollution levels in the roadside areas are increasing at an alarming rate[8,25,26].

Gautam et al.[20] reported higher variation of PM in terms of size range 10–20 μm (inhalable), 4–10 μm (thoracic) and <4 μm (alveolic) in various places of three Indian opencast mines. The results show a greater fraction of inhalable PM compared to thoracic and alveoli PM. Here we study the profile of particles of various size range in ambient air along the roadside of JCF[20]. PM samples were collected with the help of a portable GRIMM (model 1.109) aerosol spectrometer. We assessed the concentration of respirable particulates and particulate concentration with respect to occupational health, specifically inhalable, thoracic and alveoli fractions generated due to different mining activities and the movement of various types of vehicles along the roads in two different areas (mining and non-mining).

Monitoring locations were chosen to represent 'mining' (JCF) and 'non-mining' (Dhanbad city) areas to monitor of air quality along the roadside at Dhanbad. (23.80°N, 86.45°E) (Figure 1). Eight monitoring locations were selected according to IS 5182 Part-XIV (ref. 27) in the mining area of JCF along the main route from Dhanbad to Ranchi National Highway (NH-32), bypass of Jharia to Kenduadeeh road that is bounded by the open cast coal mine of JCF (Figure 1). One more location was selected to represent the non-mining area in Dhanbad city at the main gate of the Indian School of Mines (ISM), Dhanbad, along the sides of NH-32. The non-mining area was selected for comparing air quality; it is located at about 7 km northeast of JCF, covering a road network of about 25 km. These locations were selected keeping in mind the various industrial/mining and commercial activities along with vehicular load and human population in them. Table 1 provides the details of monitoring locations and their respective GPS coordinates.

PM concentration was monitored during 14–20 November 2014 (working days) at hourly frequency. Samples were collected during peak hours of traffic between 9.00 and 11.00 a.m. as well as 4.00 and 6.00 p.m. Occupational PM parameters designated as inhalable
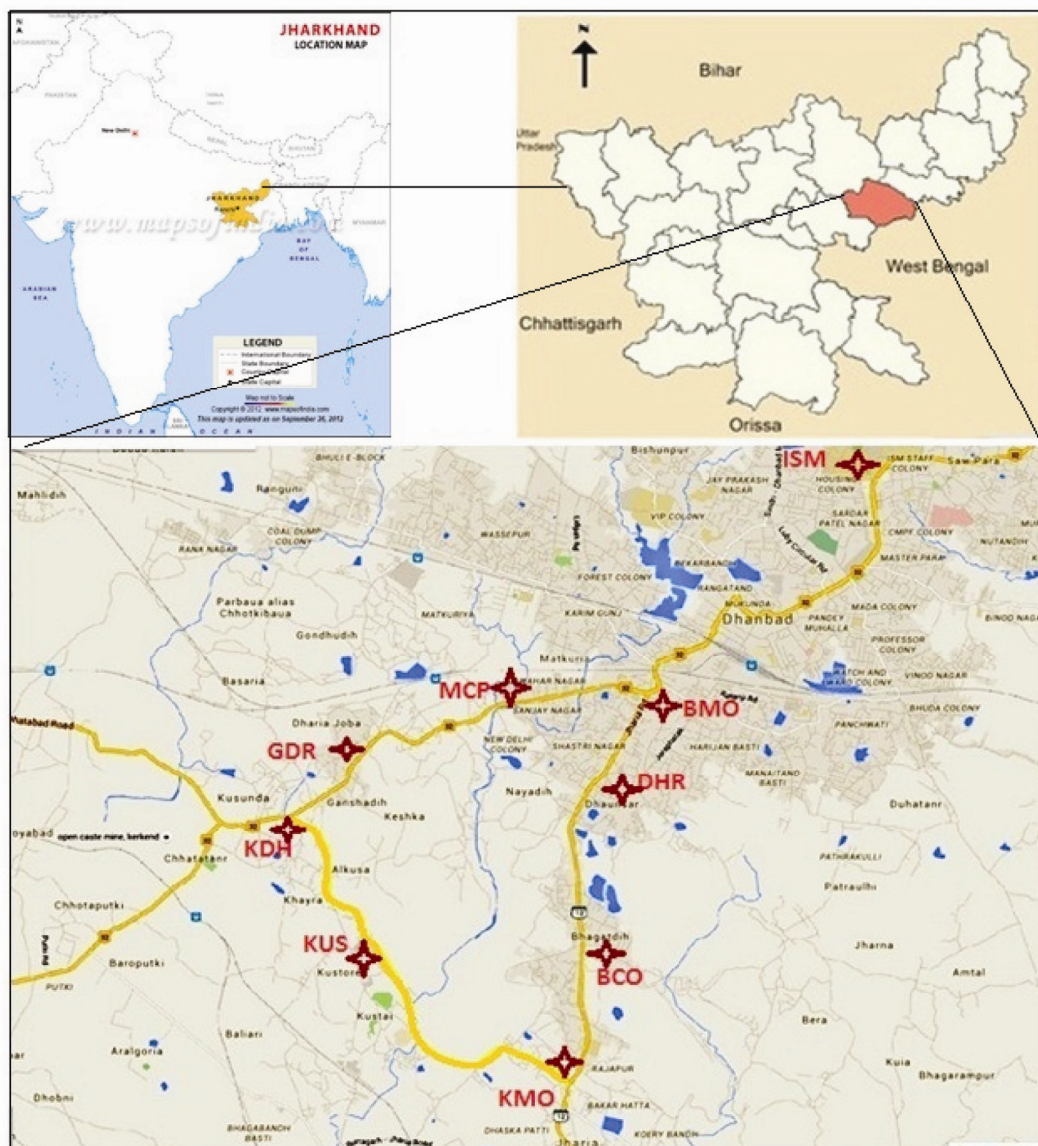
Figure 1. Map of monitoring location in the study area.

(PM$_{inhalable}$), thoracic (PM$_{thoracic}$) and alveoli (PM$_{alveoli}$) for particle size range 10–34, 4–10 and <4 µm respectively, were monitored using a portable GRIMM (model 1.109) aerosol spectrometer (GRIMM Aerosol, Technik GmbH & Co. KG, Germany; sensitivity: <1 ng m^{-3} (aerosol-dependent); reproducibility: ±3%; accuracy: 0.1 mg/m^3). The sizes of the inhalable, thoracic and alveolic particles were chosen according to the literature[20,28]. The instrument was placed at a distance up to 20 m from the centre of the road; the sampling inlet was placed at 1.2 m from the ground level and data were recorded at 1 min intervals. The instrument can directly record particle concentration and particle number count over a wide size range from 0.25 to 34 µm in 31 size channels and also in terms of inhalable, thoracic and alveoli fractions as well as simultaneously PM$_{10}$, PM$_{2.5}$ and PM$_1$, which gives a direct reading of PM concentration[29]. The instrument can also measure PM concentration with inlet flow rate of 1.2 litre min^{-1} in time intervals ranging from 6 sec to 60 min. Air enters the instrument via the sample inlet. Particles in the air sample are detected by light scattering inside the measuring cell. The scattering light pulse of each particle is counted and intensity of its scattering light signal classified to a certain particle size.

The main advantage of this instrument is direct reading of particulate concentration. Other advantages are that it is easy to operate, requires low maintenance, and has the ability to run for long periods without specific supervision over other real-time measurement instruments. The GRIMM spectrometer has been widely used to measure particle concentration in real time on hourly basis in the size range 0.23–20 µm at half hourly intervals[21,30–32].

Table 1. Details of monitoring locations and their characteristics

Location	Location ID	Coordinate		Description
		N	E	
Bankmore	BMO	23°47′18.4″	86°25′11.6″	BMO is a major junction in Dhanbad consisting of all types of activities such as commercial, residential and heavy traffic. Vehicle load is also maximum at this junction due to connection of all major roads. Mining and industrial activities are within 1 km from this junction.
Matkuria check post	MCP	23°47′14.1″	86°24′14.6″	MCP consists of residential, commercial and nearby industrial/mining activities. Load of industrial activities is predominant among activities. Traffic also consists of low and heavy vehicles.
Godhar	GDR	23°47′2.9″	86°23′43.6″	GDR consists mainly of industrial and mining activities. Few residential areas are also seen. Traffic load is medium. Load of industrial activities and heavy vehicles is predominant among activities.
Kenduadeeh	KDH	23°46′32.4″	86°22′48.8″	KDH is a junction in industrial and mining area. This point consists of commercial, residential and nearby mining activities. Vehicle load is also maximum at this junction due to connection of bypass and NH-32 roads.
Kustaur	KUS	23°45′40.5″	86°23′26.1″	KUS consists of mining, commercial and residential activities with low traffic density.
Katrasmore	KMO	23°44′54.5″	86°24′36.0″	KMO is a junction in the mining area. This point consists of commercial, residential and nearby industrial/mining activities. Vehicle load is also maximum at this junction due to connection of bypass and Jharia town roads.
Bastacola	BCO	23°45′29.1″	86°24′42.0″	BCO consists of residential, commercial and nearby industrial/mining activities. It also has medium traffic. This is the main connecting road to Jharia town.
Dhansar	DHR	23°46′43.0″	86°24′45.6″	DHR consists of commercial, residential and mining activities. It also has medium traffic. Commercial activities are predominant at this point.
ISM gate (non-mining area)	ISM	23°48′32.5″	86°26′33.6″	ISM Gate is in the non-mining area. It consists of commercial and residential activities. Traffic load is medium consisting of commercial and personal vehicles predominantly during day hours.
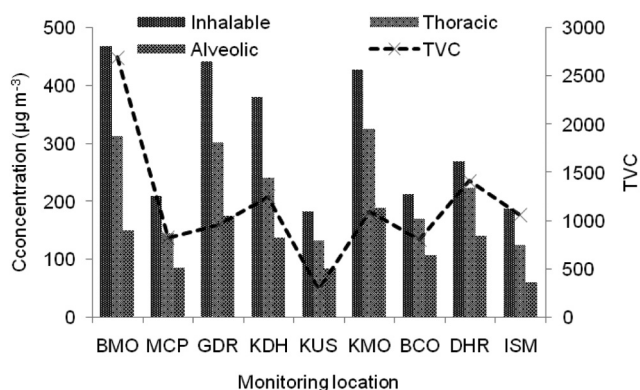
Figure 2. Variation in the concentration of inhalable, thoracic and alveolic particles with respect to TVC.

The traffic flow count was made manually on an hourly basis during the monitoring period at each selected loca-

tion. The vehicles were categorized into six groups, such as two-wheelers (2W), three-wheelers (3W), four-wheelers (4W), bus, carriers and heavy truck/Hyva truck (HT). Traffic growth from 2003–04 to 2013–14 was obtained from the Jharkhand Transport Department. The meteorological parameters, for example, temperature (°C), rainfall (mm), humidity (%), pressure (millibar), wind speed (m s^{-1}), and wind direction (degree) were collected from the weather monitoring station installed at the Department of Environmental Science and Engineering (ESE), ISM, Dhanbad during the monitoring period for correlation. Statistical parameters were calculated for each particle for various locations.

Figure 2 shows the variation in the concentration of inhalable, thoracic and alveolic particles with respect to traffic volume count (TVC). Concentration of inhalable, thoracic and alveolic particles was observed to be about three times higher compared to ISM, mainly at BMO,

GDR and KMO. Concentration of inhalable, thoracic and alveolic particles at BMO, GDR and KMO was respectively 2.5, 2.3 and 2.2 times higher than ISM. The coarse and fine particles were formed due to mining activities, heavy traffic and resuspension of road dusts near coal mining areas[21,33]. Hence the proportion of such particles was high in these regions.
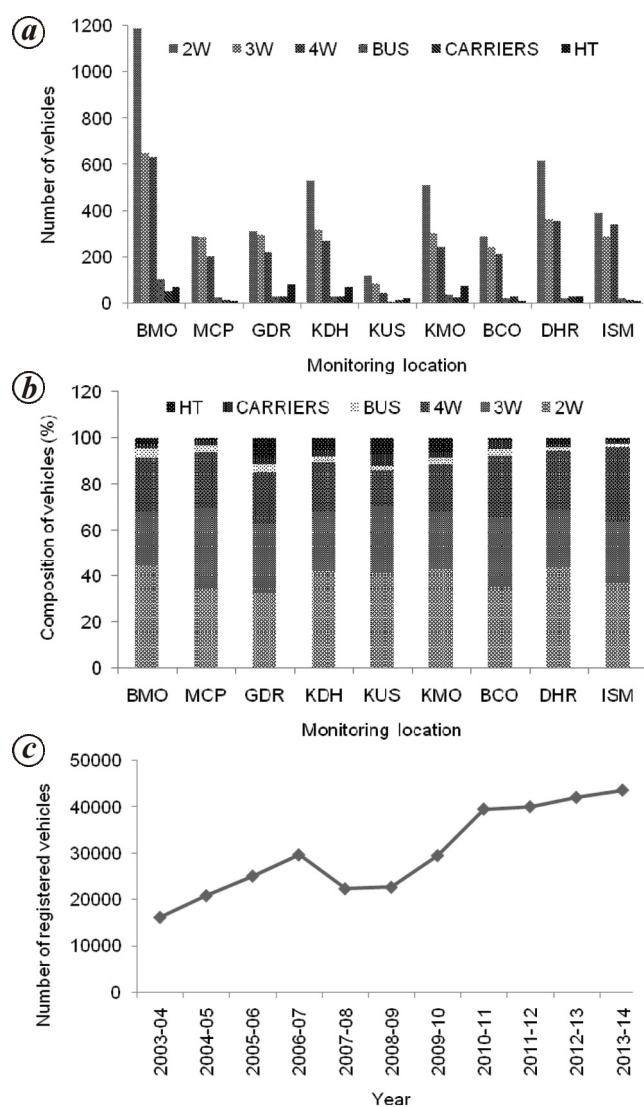
Figure 2 indicates the variation in the particle concentration with respect to TVC, except for GDR. This may due to the presence of the nearby mining area and more number of Hyva trucks. These trucks are used for transportation of coal in the mining areas. Similar studies have been made by a number of researchers[17,34].

The concentration of inhalable, thoracic and alveoli particles was higher at BMO, GDR, KDH and KMO in the mining area, which can affect human health, like eye,

Figure 3. *a*, Hourly average variation of traffic. *b*, traffic composition at each location. *c*, number of registered vehicles in Dhanbad, Jharkhand, India (source: Jharkhand Transport Office).

nose and throat irritation, coughing or wheezing, cardiopulmonary disease and headache[2,4,34].

Figure 3 *a*–*c* shows the variation of traffic, composition and growth in the number of motor vehicles in Dhanbad respectively. Traffic was monitored to strengthen the available background information on the type of vehicles generally found and the associated traffic flow patterns in the selected locations during the monitoring period. Figure 3 *a* shows hourly average traffic flow at all locations. Average traffic flow was maximum at BMO and followed by KDH, KMO and DHR. Figure 3 *b* shows a larger number of Hyva trucks at BMO, GDR, and KMO, which is the leading cause of particulate pollution in these locations. The number of two-wheelers and three wheelers was more than 50% of total traffic in all the monitoring locations. The composition of aerosols and particles depends on their source. According to the Jharkhand Transport Department, the number of vehicles on the road showed an increasing trend with time mainly during 2003–04 to 2006–07. Figure 3 *c* shows the growth of various types of registered vehicles in Dhanabd district over the last 12 years. Higher growth rate of vehicles and movement of old, larger vehicles (more than 10 years) are the major causes of air pollution in the study area along the roadsides as well as the surroundings.

Average mass concentration of inhalable, thoracic and alveoli particles was analysed statistically, from open cast coal mining as well as vehicular pollutants in mining and non-mining areas (Table 2). Concentration of inhalable particles with mean ± standard deviation, median and co-efficient of variation values for the most part BMO (467.89 ± 192.32, 465.04 μg m^{-3} and 0.41); GDR (441.77 ± 251.68, 356.04 μg m^{-3} and 0.57); and KMO (407.77 ± 156.81, 392.77 μg m^{-3} and 0.38) was around three times higher than ISM (188.16 ± 77.58, 176.24 μg m^{-3} and 0.41). The standard deviation is very high, indicating that the curves are not normal for the above locations; they are platykurtic in nature, except at DHR. Skewness shows a positive value, indicating that the distribution of curves is positively skewed, i.e. the right tail of the distribution is longer than the left tail at all locations. Concentration of thoracic particles at BMO (313.90 ± 110.20, 317.12 μg m^{-3} and 0.35), GDR (301.79 ± 126.58, 260.95 μg m^{-3} and 0.42), and KMO (309.50 ± 92.00, 300.37 μg m^{-3} and 0.30) was approximately three times higher than ISM (124.70 ± 35.39, 121.11 μg m^{-3} and 0.28). The standard deviation is very high indicating that the curves are not normal; they are platykurtic in nature, except at GDR, KDH and KUS among other locations. The distribution of the curves is positively skewed at all locations, and negatively skewed at BMO. Concentration of alveoli particles at BMO (150.07 ± 36.57, 155.36 μg m^{-3} and 0.24); GDR (174.92 ± 53.65, 157.34 μg m^{-3} and 0.31), and KMO (181.37 ± 40.79, 183.68 μg m^{-3} and 0.22) was approximately three times higher than ISM (59.99 ± 12.22,

Table 2. Statistical analysis of the concentration ($\mu g\ m^{-3}$) of inhalable, thoracic and alveolic particles

Parameter		BMO	MCP	GDR	KDH	KUS	KMO	BCO	DHR	ISM
					Monitoring location					
Inhalable particles	Average	467.89	209.36	441.77	381.45	183.43	407.77	213.29	268.99	188.16
	SD	192.32	117.91	251.68	284.20	85.56	156.81	69.40	66.64	77.58
	Median	465.04	168.24	356.04	263.87	153.08	392.77	203.78	253.84	174.24
	Skewness	0.01	1.36	1.11	1.63	1.62	0.81	0.64	1.45	1.22
	Kurtosis	−1.17	1.17	0.94	2.23	2.82	1.02	0.02	3.17	2.46
	COV	0.41	0.56	0.57	0.75	0.47	0.38	0.33	0.25	0.41
Thoracic particles	Average	313.90	144.67	301.79	241.25	132.82	309.50	171.27	224.49	124.70
	SD	110.20	49.35	126.58	116.87	38.03	92.00	42.69	36.83	35.39
	Median	317.12	131.76	260.95	193.94	121.60	300.37	164.25	221.48	121.11
	Skewness	−0.01	1.45	1.26	1.68	1.92	0.77	0.61	1.04	0.69
	Kurtosis	−0.89	2.35	1.78	2.94	4.91	0.86	−0.06	1.96	0.50
	COV	0.35	0.34	0.42	0.48	0.29	0.30	0.25	0.16	0.28
Alveolic particles	Average	150.07	86.45	174.92	137.55	83.71	181.37	108.47	140.18	59.99
	SD	36.57	14.46	53.65	45.78	15.34	40.79	21.36	13.98	12.22
	Median	155.36	83.20	157.34	122.64	78.24	183.68	101.51	138.36	58.50
	Skewness	−0.33	1.16	1.54	2.31	2.28	0.52	0.97	0.64	0.86
	Kurtosis	−0.95	1.64	2.20	6.79	6.64	0.75	0.31	0.02	0.82
	COV	0.24	0.17	0.31	0.33	0.18	0.22	0.20	0.10	0.20

SD, Standard deviation; COV, Coefficient of variation.

Table 3. Statistical correlation analysis of inhalable, thoracic and alveolic particles

	Thoracic vs inhalable		Alveolic vs inhalable		Alveolic vs thoracic	
Location	Best fit equation	R^2	Best fit equation	R^2	Best fit equation	R^2
BMO ($n = 85$)	$y = 1.586x - 29.98$	0.83	$y = 4.443x - 198.92$	0.71	$y = 2.739x - 97.14$	0.83
MCP ($n = 97$)	$y = 2.055x - 88.00$	0.74	$y = 3.080x - 56.89$	0.14	$y = 2.183x - 44.11$	0.41
GDR ($n = 97$)	$y = 1.620x - 47.37$	0.66	$y = 2.889x - 63.65$	0.38	$y = 2.103x - 66.08$	0.79
KDH ($n = 131$)	$y = 2.086x - 122.00$	0.74	$y = 3.925x - 158.50$	0.40	$y = 2.257x - 69.21$	0.78
KUS ($n = 112$)	$y = 1.873x - 65.43$	0.69	$y = 2.761x - 47.73$	0.25	$y = 1.793x - 17.28$	0.52
KMO ($n = 160$)	$y = 1.389x - 25.01$	0.81	$y = 2.594x - 62.59$	0.60	$y = 1.980x - 48.37$	0.84
BCO ($n = 84$)	$y = 1.431x - 31.94$	0.78	$y = 2.141x - 18.96$	0.43	$y = 1.780x - 21.82$	0.79
DHR ($n = 104$)	$y = 1.556x - 80.36$	0.74	$y = 2.749x - 116.49$	0.33	$y = 2.139x - 75.34$	0.66
ISM ($n = 95$)	$y = 1.707x - 24.75$	0.61	$y = 3.758x - 37.31$	0.35	$y = 2.567x - 29.32$	0.79

58.50 $\mu g\ m^{-3}$ and 0.20). The value of kurtosis is less than 3, indicating that the curve is platykurtic in nature except at GDR, KDH and KUS, where it is leptokuortic. The distribution of curves is positively skewed, except at BMO. A similar study was made recently on the exposure to inhalable, thoracic and alveolic particles with respect to various modes of transportation in Delhi[35]. Gautam *et al.*[20] reported higher variation in concentration of inhalable, thoracic and alveoli particles at various places of three Indian opencast mines.

Table 3 presents the correlation between thoracic versus inhalable, alveolic versus inhalable, and alveolic versus thoracic particles. Correlation of thoracic and inhalable was significant at all locations while alveolic and thoracic was significant at all locations except MCP. Correlation of alveolic and inhalable was maximum at BMO

and KMO in comparison to other locations. This may be due to generation of more inhalable particles in comparison to alveolic particles from road traffic. The inhalable, thoracic and alveolic particle concentration was typically higher at BMO, GDR and KMO, with better coefficient of fitness due to high traffic and mining activities.

Meteorology plays a significant role for distribution of pollutant in ambient air[36–38]. Hourly average meteorological parameters such as temperature, humidity, wind speed, atmospheric pressure, dew point and solar radiation were observed to be 23.4°C, 52.4%, 2.2 m s^{-1}, 981.8 millibar, 11.7°C and 163.9 Wm^{-2} respectively, throughout the monitoring period (Table 4). No rainfall was recorded during the monitoring period. Fractions of wind speed were found in the range 0.5–2.1 m s^{-1}, which is more than 50% during monitoring. This was significantly

slower and less than 3 m s^{-1}. The atmospheric condition was stable during the monitoring period.

Figure 4 shows the variation of inhalable, thoracic and alveolic particle mass composition at different monitoring locations. Contribution of mass in various size fractions of inhalable particles was separated by size (PM$_{inhalable–thoracic}$, PM$_{thoracic–alveolic}$ and PM$_{alveolic}$). The study showed that the dominant composition of PM$_{alveolic}$ particles was between 32% and 52% at all locations, except non-mining area, whereas PM$_{thoracic-alveolic}$ particles was between 26% and 35% at all locations. Burning of coal and coal transportation through the road are a main source of alveolic particles. Mining plays a main role in the generation of alveolic particles, mainly at KUS, KMO, BCO and DHR. The proportion of alveolic particles was observed to be higher in the study area. These particles of dust can deeply penetrate into the unciliated airways of the lung (the alveolar region) and be absorbed directly into the pulmonary circulation system[39]. Previous studies have reported that coal mining activities and movement of vehicles are the major source of generation of coarser and fine particles; the finer particles stay for a longer time in the environment[11,20]. The analysis showed that majority of alveolic mass particles fall under inhalable particles mass concentration. Earlier studies also reported similar findings[20,40].

Table 5 presents ratio of thoracic/inhalable, alveolic/thoracic and alveolic/inhalable. Ratio of thoracic/inhalable was found to be in the range 63–83% while
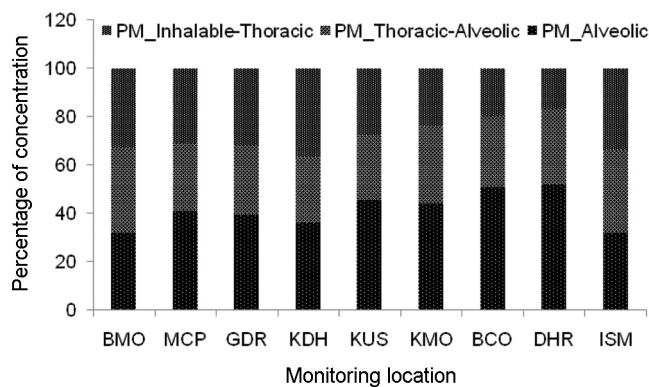
alveolic/inhalable in the range of less than 52% at all locations. Alveolic/thoracic ratio was also found to be more than 50% except BMO and ISM. This may be due to presence of coal fire, mining activities and road transportation (heavy vehicles). Similar findings have been reported earlier also[8,40,41].

Figure 5 shows particle mass concentration analysis on the basis of size (0.225–34.0 μm) at all locations. Contribution of particle size in the 0.615–1.450 μm range was found less in both types of area. Contribution of particles of size 0.375 μm and 2.750 μm was observed to be significant in mining areas; these fall in range of alveolic particles. Contribution of particle size 5.750 μm was observed to be maximum at all locations; these fall in range of thoracic particles. Contribution of particle size 22.500 μm was observed to be significant at all locations in both regions; these fall in range of inhalable particles. Contribution of particles of size 0.375 μm were almost two to three times higher than at ISM (non-mining area) at all locations. Due to heavy traffic movement and coal mining activities finer and coarse particles are generated in enormous amounts, the finer particles stays for a longer time in the environment[11]. Larger particles showed
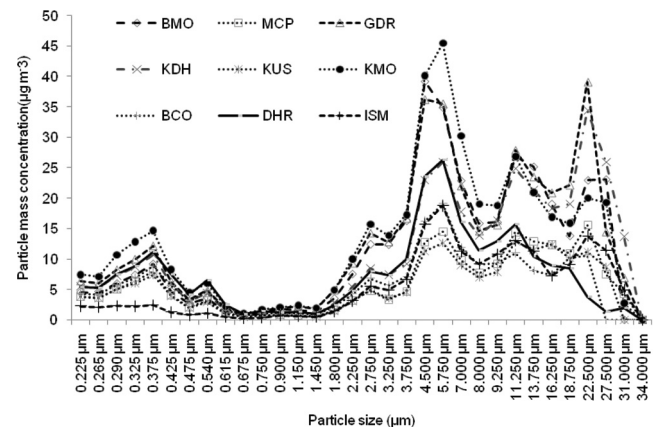

Figure 4. Percentage of particulate matter concentration in various sizes segregated in different locations.

Figure 5. Distribution of particle mass concentration according to size at all monitoring locations.

Table 4. Meteorological parameters during the monitoring period

Parameter	Mean	Minimum	Maximum	SD
T (°C)	23.7	13.6	35.4	4.7
RH (%)	52.4	18.7	81.2	15.1
WS (m s^{-1})	2.2	0.0	6.8	1.2
AP (millibar)	981.8	977.5	987.3	1.8
DP (°C)	11.7	2.1	21.6	4.0
SR (Wm^{-2})	163.9	0.0	727.7	230.9

T, Temperature; RH, Relative humidity; WS, Wind speed; AP, Atmospheric pressure; DP, Dew point and SR, Solar radiation.

Table 5. Average particulate matter (PM) (inhalable, thoracic, and alveolic) mass concentrations ratios

	PM		
Location	Thoracic/inhalable	Alveolic/thoracic	Alveolic/inhalable
BMO	0.67	0.48	0.32
MCP	0.69	0.60	0.41
GDR	0.68	0.58	0.40
KDH	0.63	0.57	0.36
KUS	0.72	0.63	0.46
KMO	0.76	0.58	0.44
BCO	0.80	0.63	0.51
DHR	0.83	0.62	0.52
ISM	0.66	0.48	0.32

higher contribution in the monitoring locations; these are more likely to get deposited in the upper airways of the lungs. Fine particles (size 0.375 and 5.750 μm) can penetrate deep into the alveolar region of the lungs, resulting in health problems. Other studies have also reported that higher pollutant levels of fine particles contribute significant negative health impacts[42,43].

The present study was conducted to analyse the variation of occupational PM (inhalable, thoracic and alveolic) along the roadsides of mining area (JCF), and non-mining area (Dhanbad city). Concentration of inhalable, thoracic and alveolic particles at BMO, GDR and KMO was respectively, 2.5, 2.3, and 2.2 times higher than at ISM (non-mining area). The distribution curves of inhalable particles were positively skewed and platykurtic in nature. In the case of thoracic and alveoli particles they were positively skewed except at BMO, where it was negatively skewed, and also platykurtic in nature, except at GDR, where it was leptokuortic in nature. Variations in particle concentration were also correlated with TVC and found to be good, except at GDR. The inhalable, thoracic, and alveolic particle concentration was higher at BMO, GDR and KMO, with better coefficient of fitness due to high traffic and mining activities.

Contribution of each type of particle at each location was also studied. Contribution of thoracic particle mass concentration out of inhalable was between 63% and 83% at all locations. Contribution of alveolic out of thoracic particles mass concentration was more than 50% at all locations, except at ISM and BMO. Contribution of alveolic out of inhalable was less than 52%, mainly at KUS, KMO, BCO and DHR. The dominant composition of $PM_{alveoli}$ particle was observed in the 32–52% range at all locations except non-mining area; while $PM_{thoracic–alveolic}$ particle was in the 26–35% range at all locations. Thus we can conclude that thoracic and inhalable particle concentration is higher at all locations in comparison to ISM, except some locations such as MCP and KUS. Alveolic particle concentration was higher at all locations in the mining area in comparison to ISM. The present study also showed that residents and local passengers are exposed to a higher concentration of occupational inhalable, thoracic and alveolic particles along the roadside mainly at BMO, GDR and KMO in the mining area.

1. Davidson, C. I., Phalen, R. F. and Solomon, P. A., Airborne particulate matter and human health: a review. *Aerosol Sci. Technol.*, 2005, **39**, 737–749.
2. Brugge, D., Durant, J. L. and Rioux, C., Near-highway pollutants in motor vehicle exhaust: a review of epidemiologic evidence of cardiac and pulmonary health risks. *Environ. Health*, 2007, **6**, 23; doi: 10.1186/1476-069X-6-236-23, doi:10.1016/j.jaerosci.2010.07.007.
3. Cao, Y. and Gao, H., Prevalence and causes of air pollution and lung cancer in Xuanwei City and Fuyuan County, Yunnan Province, China. *Front. Med.*, 2012, **6**(2), 217–220.
4. United Nations, World Urbanization Prospects 2015: The 2014 Revision, ST/ESA/SER.A/366. Department of Economic and Social Affairs, Population Division, New York; http://esa.un.org/unpd/wup/FinalReport/WUP2014-Report.pdf
5. Brook, R. D., Cardiovascular effects of air pollution. *Clin. Sci.*, 2008, **115**(6), 175–187.
6. Kurth, M. L., McCawley, M., Hendryx, M. and Lusk, S., Atmospheric particulate matter size distribution and concentration in West Virginia coal mining and non-mining areas. *J. Exp. Sci. Environ. Epidemiol.*, 2014, **24**, 405–411.
7. Marrugo-Negrete, J. L., Urango-Cardenas, I. D., Núñez, S. M. B. and Díez, S., Atmospheric deposition of heavy metals in the mining area of the San Jorge River basin, Colombia. *Air Qual. Atmos. Health*, 2014, **7**, 577–588.
8. Pandey, B., Agrawal, M. and Singh, S., Assessment of air pollution around coal mining area: emphasizing on spatial distributions, seasonal variations and heavy metals, using cluster and principal component analysis. *Atmos. Pollut. Res.*, 2014, **5**, 79–86.
9. Wrobel, A., Rokita, E. and Maenhaut, W., Transport of traffic-related aerosols in urban areas. *Sci. Total Environ.*, 2000, **257**, 199–211.
10. Charron, A., Introduction: focus on airborne particulate matter from the transport sector. *Aerosol. Sci. Technol.*, 2010, **44**, 485–486.
11. World Health Organization, Health risks of particulate matter from long-range transboundary air pollution. Joint WHO/Convention task force on the health aspects of air pollution, 2006. European Centre for Environment and Health Bonn Office. http://www.euro.who.int/__data/assets/pdf_file/0006/78657/E88189.pdf
12. Hendryx, M. and Ahern, M., Relations between health indicators and residential proximity to coal mining in West Virginia. *Am. J. Public Health*, 2008, **98**(4), 669–671.
13. Abidin, E. Z., Semple, S., Rasdi, I., Ismail, S. N. S. and Ayres, J. G., The relationship between air pollution and asthma in Malaysian school children. *Air Qual. Atmos. Health*, 2014, **7**, 421–432.
14. Ghose, M. K. and Majee, S. R., Air pollution caused by opencast mining and its abatement measures in India. *J. Environ. Manage.*, 2001, **63**(2), 193–202.
15. Chaulya, S. K., Assessment and management of air quality for an opencast coal mining area. *J. Environ. Manage.*, 2004, **70**, 1–14.
16. Naidoo, R., Seixas, N. and Robins, T., Estimation of respirable dust exposure among coal miners in South Africa. *J. Occup. Environ. Hyg.*, 2006, **3**, 293–300.
17. Bathmanabhan, S. and Saragur Madanayak, S. N., Analysis and interpretation of particulate matter – PM_{10}, $PM_{2.5}$ and PM_1 emissions from the heterogeneous traffic near an urban roadway. *Atmos. Pollut. Res.*, 2010, **1**, 184–194.
18. Srimuruganandam, B. and Shiva Nagendra, S. M., Characteristics of particulate matter and heterogeneous traffic in the urban area of India. *Atmos. Environ.*, 2011, **45**, 3091–3102.
19. Deshmukh, D. K., Deb, M. K. and Mkoma, S. L., Size distribution and seasonal variation of size-segregated particulate matter in the ambient air of Raipur city, India. *Air Qual. Atmos. Health*, 2013, **6**, 259–276.
20. Gautam, S., Kumar, P. and Patra, A. K., Occupational exposure to particulate matter in three Indian opencast mines. *Air Qual. Atmos. Health*, 2014; doi:10.1007/s11869-014-0311-6
21. Mohan, M. and Payra, S., Aerosol number concentrations and visibility during dense fog over a subtropical urban site. *J. Nanomater*, 2014, Article ID: 495457, p 6; http://dx.doi.org/10.1155/2014/495457
22. Phalen, R. F. and Mendez, L. B., Dosimetry considerations for animal aerosol inhalation studies. *Biomarkers*, 2009, **14**, 63–66; doi:10.1080/13547500902965468
23. Census of India, Jharkhand Provisional Result-Census 2011; available at: http://censusindia.gov.in/2011census/censusinfodashboard/stock/profiles/en/IND020_Jharkhand.pdf
24. Central Pollution Control Board, National Ambient Air Quality Standards (NAAQS), Gazette Notification, New Delhi, 2009.

25. Jain, M. K. and Saxena, N. C., Air quality assessment along Dhanbad–Jharia road. *Environ. Monit. Assess.*, 2002, **79**, 239–250.

26. Dubey, B., Pal, A. K. and Singh, G., Trace metal composition of airborne particulate matter in the coal mining and non-mining areas of Dhanbad Region, Jharkhand, India. *Atmos. Pollut. Res.*, 2012, **3**, 238–246.

27. IS 5182, Methods for Measurement of Air Pollution. Part 14, 2000: Guidelines for Planning the Sampling of Atmosphere (Second Revision).

28. Ruzer, L. S. and Harley, N. H., *Aerosols Handbook: Measurement, Dosimetry, and Health Effects*, CRC Press, 2004, 2nd edn, ISBN: 1439855196, 9781439855195, p. 666.

29. GRIMM, *Operation manual of Portable Laser Aerosol spectrometer and dust monitor (Model 1.108/1.109)*, GRIMM Aerosol Technik GmbH & Co. KG, Ainring, Germany, 2010.

30. Peters, T. M., Ott, D. and O'Shaughnessy, P. T., Comparison of the GRIMM 1.108 and 1.109 portable aerosol spectrometer to the TSI 3321 aerodynamic particle sizer for dry particles. *Ann. Occup. Hyg.*, 2006, **50**, 843–850.

31. Grimm, H. and Eatough, D., Aerosol measurement: the use of optical light scattering for the determination of particulate size distribution, and particulate mass, including the semi-volatile fraction. *J. Air Waste Manage. Assoc.*, 2009, **59**(1), 101–107.

32. Burkart, J., Steiner, G., Reischl, G., Moshammer, H., Neuberger, M. and Hitzenberger, R., Characterizing the performance of two optical particle counters (GrimmOPC1.108 and OPC1.109) under urban aerosol conditions. *J. Aerosol Sci.*, 2010, **41**, 953–962.

33. Sastry, V. R., Ram Chandar, K., Nagesha, K. V., Murlidhar, E. and Mohuiddin, M. S., Prediction and analysis of dust dispersion from drilling operation in opencast coal mines. *Procedia Earth Planetary Sci.*, 2015, **11**, 303–311.

34. Jo, W. K. and Park, J. H., Analysis of roadside inhalable particulate matter (PM10) in major Korean cities. *Environ. Manage.*, 2005, **36**, 826–841; doi:10.1007/s00267-004-0341-1.

35. Kumar, P. and Gupta, N. C., Commuter exposure to inhalable, thoracic and alveolic particles in various transportation modes in Delhi. *Sci. Total Environ.*, 2016, **541**, 535–541.

36. Elminir, H. K., Dependence of urban air pollutants on meteorology. *Sci. Total Environ.*, 2005, **350**, 225–237.

37. Tiwari, S., Chate, D. M., Pragya, P., Ali, K. and Bisht, D. S., Variations in mass of the PM_{10}, $PM_{2.5}$ and PM_1 during the monsoon and the winter at New Delhi. *Aerosol Air Qual. Res.*, 2012, **12**, 20–29.

38. Yadav, S., Praveen, O. D. and Satsangi, P. G., The effect of climate and meteorological changes on particulate matter in Pune, India. *Environ. Monit. Assess.*, 2015, **187**(7), 402; doi:10.1007/s10661-015-4634-z.

39. Brown, J. S., Gordon, T., Price, O. and Asgharian, B., Thoracic and respirable particle definitions for human health risk assessment. *Particle Fibre Toxicol.*, 2013, **10**, 12; http://www.particleandfibretoxicology.com/content/10/1/12

40. Niu, X., Guinot, B., Cao, H. X. and Sun, J., Particle size distribution and air pollution patterns in three urban environments in Xi'an, China. *Environ. Geochem. Health*, 2014, **37**(5), 801–812; doi:10.1007/s10653-014-9661-0.

41. Giuglino, M., Lonati, G., Butelli, P., Romele, L., Tardivo, R. and Grosso, M., Fine particulate ($PM_{2.5}$–PM_1) at urban sites with different traffic exposure. *Atmos. Environ.*, 2005, **39**, 2412–2431.

42. Duzgoren-Aydin, N., Health effects of atmospheric particulates: a medical geology perspective. *J. Environ. Sci. Health C*, 2008, **26**(1), 1–39.

43. Baccini, M., Biggeri, A., Grillo, P., Consonni, D. and Bertazzi, P. A., Health impact assessment of fine particle pollution at the regional level. *Am. J. Epidemiol.*, 2011, **174**, 12; doi:10.1093/aje/kwr256.

Nature of suspended particles in hydrothermal plume at 3°40′N Carlsberg Ridge: a comparison with deep oceanic suspended matter

Durbar Ray[1,*], E. V. S. S. K. Babu[2] and L. Surya Prakash[1,3]

[1]CSIR-National Institute of Oceanography, Dona Paula, Goa 403 004, India
[2]CSIR-National Geophysical Research Institute, Uppal Road, Hyderabad 500 007, India
[3]Present address: ESSO-National Centre for Antarctic and Ocean Research, Vasco da Gama, Goa 403 804, India

Suspended matter from hydrothermal plume at 3°40′N Carlsberg Ridge was studied for microtexture and geochemistry. Characteristics of these plume particles were compared with deep-oceanic particulates from different depths. Compared to fine, deep-oceanic suspended matter (≤2.0 μm), some particles in the plume were larger (≥20 μm) and had irregular shape and surface. These plume particles were mostly composed of Fe-oxides and silicates. Bulk composition showed that plume particles were relatively enriched with Fe, P, Mn, rare earth elements (except Ce) and U, but had other trace element concentration analogous to that found in deep-oceanic suspended matter. Efficient scavenging of elements from hydrothermal fluid and sea water makes geochemistry of plume particulates different from common oceanic particles.

BUOYANT hydrothermal fluids emanate from active vents and rise through the water column until it attains neutral buoyancy. During mixing with ambient sea water, dissolved elements in the hydrothermal fluids form metallic sulphides, sulphates, oxides and oxy-hydroxides[1,2]. Commonly, sulphides form at the buoyant stage of any hydrothermal emission, while later oxidation of reduced metals develops oxide particles in non-buoyant plume[3,4]. All these particles of hydrothermal origin are dispersed laterally along with neutrally buoyant plume following deep-sea currents. Such metal-rich hydrothermal particles make major contribution of various trace elements to the oceanic geochemical budget. However, detailed characterization of hydrothermal particles has only rarely been attempted[5].

Recently, hydrothermal plumes from unknown vent(s) were discovered near 3°40′N Carlsberg Ridge[6]. In the present study we determine the morphological and geochemical nature of these plume particles. Geochemistry

*For correspondence. (e-mail: dray@nio.org)